

# The Kuramoto model with distributed shear

DIEGO PAZÓ<sup>1</sup> and ERNEST MONTBRIÓ<sup>2</sup>

<sup>1</sup> *Instituto de Física de Cantabria (IFCA), CSIC-Universidad de Cantabria - 39005 Santander, Spain*

<sup>2</sup> *Department of Information and Communication Technologies, Universitat Pompeu Fabra - 08003 Barcelona, Spain*

PACS 05.45.Xt – Synchronization; coupled oscillators

**Abstract.** - We uncover a solvable generalization of the Kuramoto model in which shears (or nonisochronicities) and natural frequencies are distributed and statistically dependent. We show that the strength and sign of this dependence greatly alter synchronization and yield qualitatively different phase diagrams. The Ott-Antonsen ansatz allows us to obtain analytical results for a specific family of joint distributions. We also derive, using linear stability analysis, general formulae for the stability border of incoherence.

**Introduction.** – Collective synchronization is a commonly observed phenomenon in nature and in some technological applications [1–5], in which mutual interactions succeed to entrain the rhythms of a heterogeneous ensemble of self-sustained oscillators. It is mathematically captured by a prototypic minimal model put forward by Kuramoto more than thirty years ago [2, 6]. Moreover, this model is a suitable framework for the quantitative analysis of a variety of physical systems such as arrays of Josephson junctions [7] or mechanical rotors/oscillators [8–10].

The universal form of a limit-cycle close to a Hopf bifurcation led Kuramoto to analyse collective synchronization resorting to the mean-field version of the complex Ginzburg-Landau equation with disorder [6, 10, 11]:

$$\dot{z}_j = z_j[1 + i(\omega_j + q_j) - (1 + iq_j)|z_j|^2] + \frac{K}{N} \sum_{k=1}^N (z_k - z_j), \quad (1)$$

where  $z_j = \varrho_j e^{i\theta_j}$ , and  $j = 1, \dots, N \gg 1$ . Here,  $\omega_j$  is the natural frequency of the  $j$ -th oscillator, whereas  $q_j$  is the so-called shear (or nonisochronicity) that quantifies the dependence of the oscillation frequency on the amplitude. Under the assumptions that the coupling is purely diffusive ( $K$  real) and weak ( $|K|$  small), a phase reduction of eq. (1) yields [2]

$$\dot{\theta}_j = \omega_j + Kq_j + \frac{K}{N} \sum_{k=1}^N [\sin(\theta_k - \theta_j) - q_j \cos(\theta_k - \theta_j)]. \quad (2)$$

We may also cast eq. (2) in a more compact form:

$$\dot{\theta}_j = \omega_j + K \tan \beta_j - \frac{1}{\cos \beta_j} \frac{K}{N} \sum_{k=1}^N \sin(\theta_j - \theta_k + \beta_j) \quad (3)$$

with  $\tan \beta_j = q_j$  and  $|\beta_j| \leq \frac{\pi}{2}$ . Under the simplifying assumption that the shears are not distributed,  $q_j = \hat{q}$  ( $\Rightarrow \beta_j = \hat{\beta}$ ), the so-called Sakaguchi-Kuramoto model [12] is recovered (redefining  $\omega'_j = \omega_j + K \tan \hat{\beta}$ , and  $K' = K/\cos \hat{\beta}$ ). Additionally, under the more severe constraint  $q_j = 0$ , eq. (3) becomes the standard Kuramoto model [6].

The goal of this work is to perform a detailed analysis of phase equations (2) under the assumption that the natural frequency and the shear of each oscillator are drawn from a joint probability density function (PDF),  $p(\omega, q)$ . A particular case of this problem has been recently analysed assuming the parameters  $\omega$  and  $q$  to be independent random variables,  $p(\omega, q) = g(\omega)h(q)$  [13]. An interesting finding is that, if the width of the distribution  $h(q)$  exceeds a precise threshold, diffusive coupling is unable to counteract shear heterogeneity leading to a self-organized, synchronous state. This result is in sharp contrast with the well-known prediction of the Sakaguchi-Kuramoto — or the Kuramoto — model, where collective synchronization is assured at large enough  $K$  values.

How do these results translate into the case where natural frequencies and shears are statistically dependent? This is the case one may encounter when studying the synchronization of any particular class of self-sustained oscillators. Generally, model-specific parameters affect *both* the oscillator's natural frequency and shear. Therefore, heterogeneity in certain parameters will also result into heterogeneity of  $\omega$  and  $q$  with some functional or statistical dependence between them; see *e.g.*, eqs. (7) and (8) in [7] for such a situation, though the heterogeneity of  $q$  is eventually neglected to simplify the analysis. In previous work, parameter dependencies were found to influence the

effect of diffusive coupling on the variance of the ensemble's oscillator frequencies, a phenomenon called 'anomalous phase synchronization' [14].

In this Letter, we define a conditional probability of  $\omega$  given  $q$ ,  $g_c(\omega|q)$ , such that  $p(\omega, q) = h(q)g_c(\omega|q)$ . The marginal PDF  $h(q)$  is assumed to be unimodal, symmetric and centred at  $q_0$ . Additionally, the conditional probability  $g_c$  is chosen to be unimodal and of the form  $g_c(\omega|q) = g_c(\omega - mq)$ . This restricts our results to a particular class of distributions that is nonetheless wide enough to illustrate a number of different synchronization scenarios (particularly depending on the sign of  $m$ ).

**Continuum limit.** — In our theoretical analysis we neglect finite-size effects and consider the thermodynamic limit  $N \rightarrow \infty$  of model (2). It is possible then to drop the indices and define the probability density for the phases  $f(\theta, \omega, q, t)$ . Thus  $f(\theta, \omega, q, t) d\theta d\omega dq$  is the ratio of oscillators at time  $t$  with phases between  $\theta$  and  $\theta + d\theta$ , natural frequencies between  $\omega$  and  $\omega + d\omega$ , and shear between  $q$  and  $q + dq$ . The density function  $f$  obeys the continuity equation

$$\partial_t f = -\partial_\theta \left( \left\{ \omega + Kq + \frac{K}{2i} [re^{-i\theta}(1 - iq) - \text{c.c.}] \right\} f \right), \quad (4)$$

where c.c. stands for complex conjugate of the preceding term, and the complex order parameter  $r$  is

$$r(t) \equiv Re^{i\Psi} = \iint_{-\infty}^{\infty} \int_0^{2\pi} e^{i\theta} f(\theta, \omega, q, t) d\theta d\omega dq. \quad (5)$$

The mean field  $r$  measures the degree of synchronization of the system. If the oscillators are uniformly distributed, a state commonly referred to as incoherence,  $f(\theta, \omega, q, t)$  equals  $p(\omega, q)(2\pi)^{-1}$ , and  $r$  vanishes. States for which part or all of the population is entrained at a given frequency result in a nonuniform distribution of the phases such that  $R > 0$ .

The density function  $f(\theta, \omega, q, t)$  is real and  $2\pi$ -periodic function in the  $\theta$  variable with the Fourier expansion

$$f(\theta, \omega, q, t) = \frac{p(\omega, q)}{2\pi} \sum_{l=-\infty}^{\infty} f_l(\omega, q, t) e^{il\theta} \quad (6)$$

where  $f_l = f_{-l}^*$ ,  $f_0 = 1$ . Inserting this Fourier series into the continuity equation (4), an infinite set of integro-differential equations for the Fourier modes is obtained:

$$\partial_t f_l = -il(\omega + Kq) f_l + \frac{Kl}{2} [r^*(1 + iq) f_{l-1} - r(1 - iq) f_{l+1}] \quad (7)$$

Note that the order parameter (5) is only determined by the first Fourier mode:

$$r^*(t) = \iint_{-\infty}^{\infty} p(\omega, q) f_1(\omega, q, t) d\omega dq. \quad (8)$$

**Ott-Antonsen ansatz.** — Recently Ott and Antonsen (OA) found an ansatz [15], which is generically [16,17] satisfied by the asymptotic dynamics of the Kuramoto model ( $q = 0$ )—and, remarkably, of many variations of it, see *e.g.* [13,18–21]. In our case this ansatz takes the form

$$f_l(\omega, q, t) = \alpha(\omega, q, t)^l \quad (9)$$

This defines a family of solutions of eq. (7) with the constraint that  $\alpha$  satisfies

$$\partial_t \alpha = -i(\omega + Kq)\alpha + \frac{K}{2} [r^*(1 + iq) - r(1 - iq)\alpha^2]. \quad (10)$$

Our simulations indicate that the asymptotic solutions of the system indeed belong to the OA manifold.

We consider first a family of joint PDFs  $p(\omega, q) = h(q)g_c(\omega|q)$ , with Lorentzian (Cauchy) marginal distribution  $h$ :

$$h(q) = \frac{\gamma/\pi}{(q - q_0)^2 + \gamma^2}, \quad (11)$$

and Lorentzian conditional distribution  $g_c$ :

$$g_c(\omega|q) = \frac{\delta/\pi}{[\omega - \omega_0 - m(q - q_0)]^2 + \delta^2}. \quad (12)$$

The specific family of PDFs defined by eqs. (11) and (12) allows us to obtain simple low-dimensional ordinary differential equations for the order parameter dynamics, and to tune the statistical dependence between  $\omega$  and  $q$  with the parameter  $m$ . (The case  $m = 0$ — $\omega$  and  $q$  independent random variables—was already addressed in [13].) In the limiting case  $\delta \rightarrow 0$ ,  $g_c$  becomes a Dirac's delta, and this results in a (deterministic) linear relationship:  $\omega = \omega_0 + m(q - q_0)$ . The terms  $r$  and  $r^*$  in eq. (10) can be evaluated by means of the residue's theorem inserting the PDFs (11) and (12) in eq. (8), and closing the integration paths in the complex plane. Concerning variable  $\omega$ , the integration must be done in the lower half complex  $\omega$ -plane because  $\alpha$  can be analytically continued in that region, as occurs in the Kuramoto model, see [15] for details. In partial fractions  $g_c(\omega|q) = (2\pi i)^{-1} \{ [\omega - \omega_0 - m(q - q_0) - i\delta]^{-1} - [\omega - \omega_0 - m(q - q_0) + i\delta]^{-1} \}$ , and the integration over  $\omega$  in eq. (8) involves only the value of  $\alpha$  at the pole  $\omega^p = \omega_0 - m(q - q_0) - i\delta$ , see [15]. Hence, eq. (8) becomes in this particular instance

$$r^*(t) = \int_{-\infty}^{\infty} h(q) \alpha(\omega = \omega^p, q, t) dq. \quad (13)$$

To evaluate this integral over  $q$  we must proceed more cautiously to warrant that  $\alpha$  can be analytically extended into the suitable half  $q$ -plane ( $q = q_r + iq_i$ , with either  $q_i \geq 0$  or  $q_i \leq 0$ ). Equation (10) for  $\alpha$  at  $(\omega^p, q)$  is:

$$\begin{aligned} \partial_t \alpha = & -i[\omega_0 - m q_0 + q(m + K) - i\delta] \alpha \\ & + \frac{K}{2} [r^*(1 + iq) - r(1 - iq)\alpha^2] \end{aligned} \quad (14)$$

If  $\alpha = |\alpha|e^{-i\psi}$  is analytic, it satisfies the Cauchy-Riemann conditions, and this can be demonstrated to imply  $\partial_{q_r} |\alpha| +$

$\partial_{q_i}|\alpha| \geq 0$ . In consequence, the maximum of  $|\alpha|$  is necessarily located on the boundary (namely, on the integration contour). Under the assumption that  $\alpha$  is analytic at  $t = 0$ , analyticity will hold for all  $t > 0$  if  $\alpha$  remains finite because  $\alpha$  is the solution of the ordinary differential equation (10) (see Theorem 8.4 in Chapt. 1 of [22]). Moreover we require  $|\alpha| \leq 1$  everywhere in the selected half complex  $q$ -plane; otherwise the Fourier modes diverge, see eq. (9). After some algebra, one finds that on the real  $q$ -axis, eq. (14) yields:

$$\partial_t|\alpha| = -\delta|\alpha| + \frac{K}{2} \operatorname{Re} [r^* e^{i\psi} (1 + iq)] (1 - |\alpha|^2), \quad (15)$$

which gives  $\partial_t|\alpha| = -\delta < 0$  at  $|\alpha| = 1$ . This implies that if  $|\alpha| \leq 1$  at  $t = 0$ , this will hold for all  $t < 0$ . On the contour closing at infinity  $q = |q|e^{i\vartheta}$  with  $|q| \rightarrow \infty$ , the dominant contributions (of order  $|q|$ ) at  $|\alpha| = 1$  give:

$$\partial_t|\alpha| = [m + K(1 - R \cos \chi)] |q| \sin \vartheta, \quad (16)$$

where  $\chi = \psi(q, t) - \Psi(t)$ . If  $\partial_t|\alpha| < 0$  is fulfilled in either  $\vartheta \in (0, \pi)$  or  $\vartheta \in (-\pi, 0)$ , we can safely choose that path for the contour closing in the integration of (13). The problem now is that if  $m \neq 0$  there are values of  $K$  in eq. (16) where the desired relation  $\partial_t|\alpha| < 0$  cannot be fulfilled due to the “uncontrolled” angle  $\chi$ . Instead of ignoring those parameter values we shall make the assumption that solutions in the range  $R < R_\times$  where  $\partial_t|\alpha| < 0$  at  $|\alpha| = 1$  is fulfilled (choosing the appropriate half-plane), can be correctly studied within this framework. Thus, eq. (16) dictates that the analysable range of  $R$  is bounded by

$$R_\times = \min(1, |1 + m/K|), \quad (17)$$

what in particular implies that, in principle, the stability of incoherence ( $R = 0$ ) can be always determined, save at  $K = -m$  ( $R_\times = 0$ ). We must take  $\vartheta \in (-\pi, 0)$  if  $m + K > 0$ , and  $\vartheta \in (0, \pi)$  if  $m + K < 0$ , for the closing of the integration contour in eq. (13). Thus, the order parameter is determined by the value of  $\alpha$  at the poles

$$r^*(t) = \alpha(\omega = \omega^p, q = q^p, t), \quad (18)$$

with  $q^p = q_0 - i\gamma$  for  $m + K > 0$ , and  $q^p = q_0 + i\gamma$  for  $m + K < 0$ . Equation (18) yields the relations  $R(t) = |\alpha(\omega^p, q^p, t)|$  and  $\Psi(t) = \psi(\omega^p, q^p, t)$ , and hence it suffices to study eq. (10) at  $(\omega, q) = (\omega^p, q^p)$ .

Recalling that  $q^p = q_0 \mp i\gamma$ , and  $\omega^p = \omega^0 + m(q^p - q_0) - i\delta$ , we obtain that the modulus and the phase of the order parameter (inside the OA manifold) obey Stuart-Landau equations:

$$\dot{R} = \left[ -\delta \mp m\gamma + \frac{K}{2}(1 \mp \gamma)(1 - R^2) \right] R \quad (19)$$

$$\dot{\Psi} = \omega_0 + \frac{K}{2}q_0(1 - R^2) \quad (20)$$

Remarkably, the radial dynamics does not depend on  $q_0$ , something that stems from the peculiarities (pointed out in [13]) of the Lorentzian distribution.

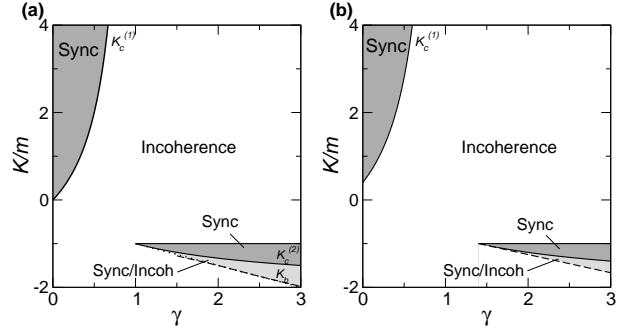


Fig. 1: Phase diagrams for positive dependence between  $\omega$  and  $q$ : eq. (12) with  $m > 0$ . (a) Purely linear dependence  $\delta = 0$ . (b)  $\delta = 0.2m$ . The solid lines correspond to the loci of bifurcations given by the analytic formulas (21), (23), and  $K = m$  (see text). The dotted line is a bound of the region of bistability given by eq. (24). Dashed lines are obtained from numerical simulations with  $N = 2000$  (a), 40000 (b) oscillators. Our numerics showed good agreement with boundaries (21) and (23), data not shown. In the simulations we took  $\{\omega_j, q_j\}_{j=1, \dots, N}$  deterministically to represent  $p(\omega, q)$  given by eqs. (11) and (12); the selected parameters were  $m = 1$  and  $\omega_0 = q_0 = \frac{1}{2}$ .

In the incoming paragraphs we present separately the cases of positive and negative  $m$ , as these two cases yield qualitatively different results.

**Positive dependence ( $m > 0$ ).** – In this case, eq. (17) implies  $R_\times = 1$  for  $K/m \geq -\frac{1}{2}$ , and  $R_\times < 1$  for  $K/m < -\frac{1}{2}$ . In the latter region we cannot solve the problem completely within the OA framework because possible attractors with  $R \in [R_\times, 1]$  are not captured by the theory.

If  $K > -m$ , the signs “ $\mp$ ” in eq. (19) must be replaced by “ $-$ ”. It can be easily seen that incoherence is stable everywhere, except above the line:

$$K_c^{(1)} = \frac{2(m\gamma + \delta)}{1 - \gamma} \quad \text{with } \gamma < 1 \quad (21)$$

A phase diagram for two values of  $\delta$  can be seen in fig. 1. At  $K_c^{(1)}$  a supercritical bifurcation gives rise to a partially synchronized solution with

$$R^2 = \frac{K - K_c}{K}. \quad (22)$$

Remarkably, this formula coincides with the one obtained in the standard Kuramoto model [2] (recovered at  $\gamma = q_0 = 0$ ).

If  $K < -m$ , one must replace “ $\mp$ ” by “ $+$ ” in eq. (19). The resulting equation predicts the incoherence to be unstable in the wedge-shaped region between  $K = -m$  and

$$K_c^{(2)} = -\frac{2(m\gamma - \delta)}{1 + \gamma} \quad \text{with } \gamma > 1 + \frac{2\delta}{m}. \quad (23)$$

If  $\omega$  and  $q$  are let to be progressively less statistically dependent ( $m \rightarrow 0$ ), the tip of this region goes to  $\gamma = \infty$ . Thus, the interval of  $\gamma$  where incoherence is stable for all

$K$  becomes infinite as  $m \rightarrow 0$ , in consistence with our result in [13] for the independent case ( $m = 0$ ). Inside the wedge-like region where incoherence is unstable we can presume—and confirm numerically—the existence of a stable partially synchronized solution (with  $R \geq R_\times$ ). Moreover, as the instability of incoherence at  $K_c^{(2)}$  is subcritical, we can infer the existence of a region of bistability incoherence-synchronization below this line. The unstable solution with  $R > 0$  appearing at  $K_c^{(2)}$  can be analytically determined up to

$$K_b = -\frac{m^2(1+\gamma)}{2(m+\delta)} \quad (24)$$

where it acquires an  $R$  larger than  $R_\times$ . Hence  $K_b$  is a bound (surprisingly tight) for the region of bistability, see fig. 1.

**Negative dependence ( $m < 0$ ).**— In the case of negative  $m$ , eq. (17) tells us that our eqs. (19) and (20) apply to all  $R$  values when  $K/|m| \leq \frac{1}{2}$ , while otherwise their validity only holds in a certain range  $R < R_\times$ . In contrast to the case of positive  $m$ , the phase diagram undergoes several transformations as the ratio between  $\delta$  and  $|m|$  varies. Next we describe the three main situations separately, see fig. 2.

*Case I:*  $0 \leq \delta < |m|/2$ ; fig. 2(a,b). If  $K > |m|$  incoherence is stable only above the line

$$K_c^{(1)} = \frac{2(-|m|\gamma + \delta)}{1 - \gamma}, \quad \text{with } \gamma > 1 \quad (25)$$

where an unstable solution branches off incoherence obeying relation (22). As presumable, a region of bistability between incoherence and synchronization (with  $R \geq R_\times$ ) is found. For  $K < |m|$  incoherence is stable everywhere except above the line

$$K_c^{(2)} = \frac{2(|m|\gamma + \delta)}{1 + \gamma}, \quad \text{with } \gamma < 1 - \frac{2\delta}{|m|} \quad (26)$$

where it undergoes a supercritical bifurcation.

Our numerical simulations reveal that a stable coherent solution exists below  $K/|m| = 1$  in the region of stable incoherence, see bottom panels of fig. 2(a,b). For  $\delta = 0$ , this solution is continuation of a fully synchronized solution existing at  $K/|m| = 1$  with  $R = \int_{-\infty}^{\infty} h(q)(1+q^2)^{-1/2} dq$ . This solution depends on  $|q_0|$ , and in consequence the region of bistability is also  $|q_0|$ -dependent. The bifurcation scenario is consistent with two saddle-node (SN) bifurcations emanating from a (codimension-2) cusp point.

*Case II:*  $|m|/2 < \delta < |m|$ ; fig. 2(c). The only relevant bifurcating lines (in addition to  $K = |m|$ ) are given by  $K_c^{(1)}$  in eq. (25) with a left branch emanating from the  $K$ -axis and existing up to  $\gamma = 2\delta/|m| - 1$ , and a right branch existing above  $\gamma = 1$ . At the left branch of  $K_c^{(1)}$  the bifurcation from incoherence is supercritical, while it is subcritical at the right branch.

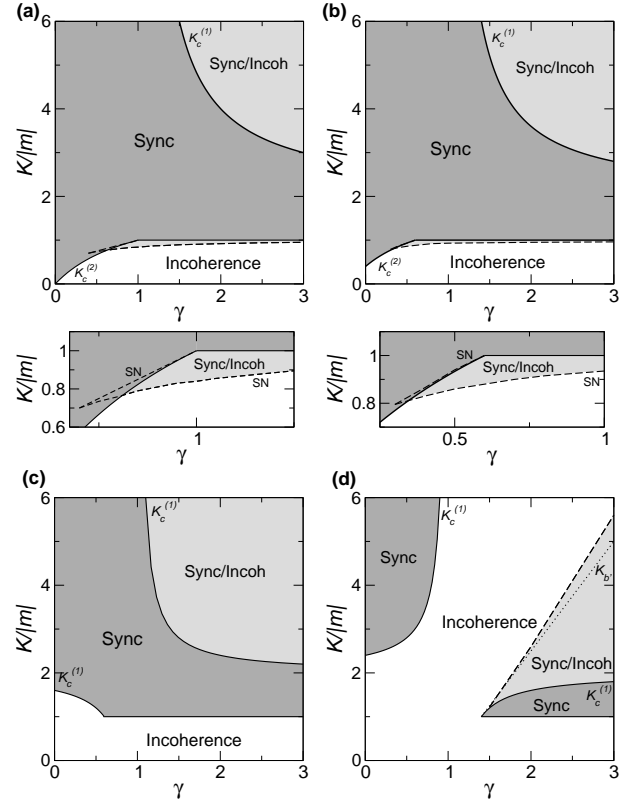


Fig. 2: Phase diagram for  $m < 0$  with  $\delta = 0$  (a),  $0.2|m|$  (b),  $0.8|m|$  (c), and  $1.2|m|$  (d). Solid lines are analytical predictions (tested by numerical simulations). The dashed lines are obtained directly from numerical simulations with  $m = -1$ ,  $q_0 = \frac{1}{2}$  and  $N = 2000$ . The dotted line in panel (d) is a bound of the region of bistability given by eq. (27). Small panels show magnified regions of the the phase diagrams (a) and (b).

*Case III:*  $\delta > |m|$ ; fig. 2(d). At  $\delta = |m|$  the locus of  $K_c^{(1)}$  [eq. (25)] reorganizes giving rise to the phase diagram for  $\delta > |m|$  shown in fig. 2(d). A wedge-like region of unstable incoherence between  $K_c^{(1)}$  and  $K = |m|$  exist above  $\gamma = 2\delta/|m| - 1$ . This means that in the limit  $m \rightarrow 0^-$  this region disappears and the phase diagram becomes the one found in [13] in the independent case ( $m = 0$ ), as expected. The fact that the right branch of  $K_c^{(1)}$  corresponds to a subcritical bifurcation results in a region of bistability. This region cannot be analytically determined, though a lower bound for its upper border can be calculated finding where an unstable solution (with  $0 < R < R_\times$ ) exists. We obtain the line

$$K_{b'} = \frac{m^2(1-\gamma)}{2(|m|-\delta)} \quad \text{with } \gamma > \frac{2\delta}{|m|} - 1 \quad (27)$$

shown as a dotted line in fig. 2(d), which is a good estimation of the upper border of the bistable region.

Remarkably, the phase diagrams for negative dependence differ significantly from those obtained for positive dependence (fig. 1). With negative  $m$ , synchrony becomes more dominant in the phase diagram, in consonance with

the numerical observations made in [14].

**Linear stability analysis.** – With general distributions the residue's theorem cannot be used. We can nevertheless follow Strogatz and Mirollo [23] and calculate the linear stability threshold of the incoherent state. This allows to know how much our results for the Lorentzian  $h(q)$  are applicable to other distributions, what is always a concern when applying the OA theory [13, 21]. Our analysis is not completely rigorous but permits to understand the results of the numerical simulations.

In the incoherent state, all Fourier modes (save  $f_0$ ) vanish:  $f_{l \neq 0} = 0$ . Equations (7) for the Fourier modes indicate that at the lowest order only the first Fourier mode  $l = \pm 1$  is relevant, and it obeys:

$$\begin{aligned} \frac{\partial f_1}{\partial t} = & -i(\omega + qK)f_1 \\ & + \frac{K}{2}(1+iq) \iint_{-\infty}^{\infty} f_1(\omega', q', t) p(\omega', q') d\omega' dq' \end{aligned} \quad (28)$$

The linear operator in the right hand side has a linear spectrum of eigenvalues  $\lambda$ . If  $f_1(\omega, q, t) = b(\omega, q) \exp(\lambda t)$  is inserted into eq. (28) and the trivial solution  $b = 0$  is discarded, we get:

$$\frac{2}{K} = \iint_{-\infty}^{\infty} \frac{1+iq}{\lambda + i(\omega + qK)} p(\omega, q) d\omega dq \quad (29)$$

Defining  $\lambda = \lambda_r + i\lambda_i$ , one finds that the imaginary part of eq. (29) has always a solution  $\lambda_i = -\omega_0$  at the stability threshold ( $\lambda_r \rightarrow 0^+$ ) if the distribution  $h(q)$  is centred at zero. As an important example, let us mention the case of Gaussian PDFs:

$$h(q) = \frac{1}{\sqrt{2\pi\nu}} e^{-\frac{q^2}{2\nu^2}}, \quad g_c(\omega|q) = \frac{1}{\sqrt{2\pi\sigma}} e^{-\frac{(\omega - \omega_0 - mq)^2}{2\sigma^2}}.$$

(hereafter we take  $\omega_0 = 0$  as this can always be achieved going into a rotating framework). We obtain an equation for the stationary ( $\lambda_i = 0$ ) instability of incoherence:

$$\frac{2}{K_c^s} = \sqrt{\frac{\pi}{2\nu^2(K_c^s + m)^2 + 2\sigma^2}} + \frac{\nu^2(K_c^s + m)}{\nu^2(K_c^s + m)^2 + \sigma^2} \quad (30)$$

For  $m = 0$  a simple analytic solution for  $K_c^s$  can be found [13]; otherwise  $K_c^s$  is the solution of a fourth-order polynomial. In the next section we show that sometimes complex eigenvalues ( $\lambda_i \neq 0$ ) may also destabilize incoherence, and hence using eq. (30) we take the risk of missing nonstationary instabilities.

**Linear dependence between  $\omega$  and  $q$ .** – If there exists a purely linear dependence of  $\omega$  on  $q$ ,  $\omega_j = m(q_j - q_0)$ , general expressions for the stability threshold of incoherence can be obtained if  $q_0 = 0$ . With this latter choice the system possesses reflection symmetry  $(\theta_j, \omega_j, q_j) \rightarrow (-\theta_j, -\omega_j, -q_j)$ , in addition to the rotational symmetry  $\theta_j \rightarrow \theta_j + \phi$ . Inserting the pdf  $p(\omega, q) = h(q)\delta(\omega - mq)$  into eq. (29), and taking the limit  $\lambda_r \rightarrow 0^+$ , we obtain:

$$\frac{2}{K_c^s} = \frac{\pi h(0)}{|K_c^s + m|} + \frac{1}{K_c^s + m}. \quad (31)$$

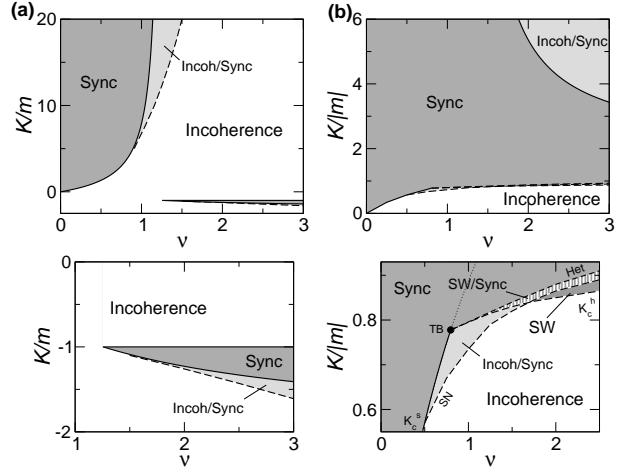


Fig. 3: Phase diagrams of model (2) with Gaussian  $h(q)$  and  $g_c = \delta(\omega - mq)$  for  $m > 0$  (a) and  $m < 0$  (b). Solid lines (numerically tested) correspond to eq. (32) [and  $K = -m$  in (a)]. Dashed lines are obtained from numerical simulations with  $|m| = 1$  and  $N = 4000$ . Small panels show magnified regions of the phase diagrams (a) and (b).

Solving this equation for  $K_c^s$  gives the boundaries:

$$K_c^s = \begin{cases} \frac{2m}{\pi h(0) - 1} & \text{if } K_c^s > -m, \\ \frac{-2m}{\pi h(0) + 1} & \text{if } K_c^s < -m. \end{cases} \quad (32)$$

The linear stability analysis permits to determine at which side of the bifurcation the incoherent state is unstable. This is an indirect indication that there must exist a horizontal bifurcation line at  $K = -m$ , exactly like in figs. 1(a) and 2(a) for Lorentzian  $h(q)$ . Moreover eq. (32) agrees with the analytical and numerical results obtained in figs. 1(a) and 2(a) for positive and negative  $m$ , respectively. Note also that reflection symmetry makes the stationary instability at  $K_c^s$  to be a (circle-)pitchfork bifurcation. We also report next the results obtained with Gaussian  $h(q)$ :

**Positive  $m$ .** The result of our numerical simulations with Gaussian  $h(q)$  and  $m > 0$  is presented in fig. 3(a), and confirms the soundness of eq. (32). In contrast to the case of Lorentzian  $h(q)$  in fig. 1(a), a region of bistability between synchronization and incoherence exists at large  $K$ . This can be understood taking the limit  $K \rightarrow \infty$ , in eq. (2) and performing a self-consistence analysis à la Kuramoto, see [13]. A solution branches off from incoherence at  $\pi h(0) = 1$  increasing the value of  $\nu$ , a scenario of subcritical bifurcation coherent with the observed bistability. The orientation of this branch is intrinsic to the form of  $h(q)$  and is independent of the value of  $m$ . For distributions with a sharp peak, like the triangular or Laplace distributions, the bifurcation is supercritical [and the phase diagram will be slightly different from that in fig. 3(a)]. The Lorentzian distribution is marginal and finite- $K$  effects make the bifurcation to be supercritical for  $m \geq 0$  and subcritical for  $m < 0$ .

*Negative  $m$ .* The numerical results for Gaussian  $h(q)$ , shown in fig. 3(b), indicate that eq. (32) predicts everywhere the correct boundaries for stable incoherence, except in a region close to  $K = |m|$  (see bottom panel). There incoherence undergoes a Hopf bifurcation at  $K_c^h$ , a bifurcation line that emanates from a double zero eigenvalue (Takens-Bogdanov) point located on  $K_c^s$  at  $\nu_{TB} = \sqrt{2/\pi}$ . (This stems from a degeneracy at  $\pi h(0) = -\int h'(q)q^{-1}dq$ .) It is remarkable that the Hopf bifurcation gives rise to a standing wave (SW) consisting of two counter-rotating clusters of locked oscillators. In the standard Kuramoto model the SW cannot arise in unimodal distributions of  $\omega$ , but it is typical of bimodal distributions with well separated peaks [5,19,20]. The other lines in the bottom panel of fig. 3(b) are (twin) saddle-node bifurcations (SN) emanating from a degenerate-pitchfork point, and a heteroclinic connection (Het) born at TB.

Taking  $q_0 \neq 0$  breaks the reflection symmetry and the phase diagram should exhibit structures already found in the Kuramoto model with bimodal non-symmetric distribution [24] or unbalanced interacting subpopulations [25].

**Conclusions.** — Our work is a natural step in the development, initiated by Winfree and Kuramoto, of realistic solvable phase models, as simplifications of the mean-field complex Ginzburg-Landau equation [6,12] or in other setups [1,26,27]. The model analysed in this Letter widens the scope of the Kuramoto model by admitting shear diversity. Shear is a generic feature of oscillators with particular relevance in ensembles of limit-cycles close to collision with a saddle point (saddle-loop bifurcation) [28]. These systems may be good candidates to observe the phenomena reported here.

Considering a broad but still reasonably simple family of joint distributions  $p(\omega, q)$ , we have found that the sign and magnitude of  $m$ , controlling the dependence between the natural frequencies and the shears, has a profound impact on the phase diagrams. Synchronization is prevalent for negative  $m$ , whereas incoherence prevails if  $m$  is positive (or zero [13]). A certainly interesting line of future work would be to investigate the effect of other dependences between  $\omega$  and  $q$  on the synchronization phase diagrams.

Finally, this work can also give hints about the validity of the OA ansatz in systems with distributed parameters [29]. Why distributing  $q$  is so amenable to analysis?

\*\*\*

Financial support from the MICINN (Spain) under project No. FIS2009-12964-C05-05 is acknowledged.

## REFERENCES

- [1] WINFREE A. T., *J. Theor. Biol.*, **16** (1967) 15.
- [2] KURAMOTO Y., *Chemical Oscillations, Waves, and Turbulence* (Springer-Verlag, Berlin) 1984.
- [3] PIKOVSKY A. S., ROSENBLUM M. G. and KURTHS J., *Synchronization, a Universal Concept in Nonlinear Sciences* (Cambridge University Press, Cambridge) 2001.
- [4] MANRUBIA S. C., MIKHAILOV S. S. and ZANETTE D. H., *Emergence of Dynamical Order* (World Scientific, Singapore) 2004.
- [5] ACEBRÓN J. A. *et al.*, *Rev. Mod. Phys.*, **77** (2005) 137.
- [6] KURAMOTO Y., *Self-entrainment of a population of coupled non-linear oscillators in International Symposium on Mathematical Problems in Theoretical Physics*, edited by ARAKI H., Vol. 39 of *Lecture Notes in Physics* (Springer, Berlin) 1975 pp. 420–422.
- [7] WIESENFELD K., COLET P. and STROGATZ S. H., *Phys. Rev. Lett.*, **76** (1996) 404.
- [8] UCHIDA N. and GOLESTANIAN R., *EPL*, **89** (2010) 50011.
- [9] MERTENS D. and WEAVER R., *Phys. Rev. E*, **83** (2011) 046221.
- [10] CROSS M. C. *et al.*, *Phys. Rev. Lett.*, **93** (2004) 224101; *Phys. Rev. E*, **73** (2006) 036205.
- [11] AIZAWA Y., *Prog. Theor. Phys.*, **56** (1976) 703. SHIINO M. and FRANKOWICZ M., *Phys. Lett. A*, **136** (1989) 103. MATTHEWS P. C. and STROGATZ S. H., *Phys. Rev. Lett.*, **65** (1990) 1701. MATTHEWS P. C., MIROLLO R. E. and STROGATZ S. H., *Physica D*, **52** (1991) 293. DE MONTE S. and D'OIDIO F., *Europhys. Lett.*, **58** (2002) 21.
- [12] SAKAGUCHI H. and KURAMOTO Y., *Prog. Theor. Phys.*, **76** (1986) 576.
- [13] MONTBRIÓ E. and PAZÓ D., *Phys. Rev. Lett.*, **106** (2011) 254101.
- [14] BLASIUS B., MONTBRIÓ E. and KURTHS J., *Phys. Rev. E*, **67** (2003) 035204. MONTBRIÓ E. and BLASIUS B., *Chaos*, **13** (2003) 291.
- [15] OTT E. and ANTONSEN T. M., *Chaos*, **18** (2008) 037113.
- [16] OTT E. and ANTONSEN T. M., *Chaos*, **19** (2009) 023117.
- [17] OTT E., HUNT B. R. and ANTONSEN T. M., *Chaos*, **21** (2011) 025112.
- [18] LEE W. S., OTT E. and ANTONSEN T. M., *Phys. Rev. Lett.*, **103** (2009) 044101. HONG H. and STROGATZ S. H., *Phys. Rev. Lett.*, **106** (2011) 054102.
- [19] MARTENS E. A. *et al.*, *Phys. Rev. E*, **79** (2009) 026204.
- [20] PAZÓ D. and MONTBRIÓ E., *Phys. Rev. E*, **80** (2009) 046215.
- [21] LAFUERZA L. F., COLET P. and TORAL R., *Phys. Rev. Lett.*, **105** (2010) 084101.
- [22] CODDINGTON E. A. and LEVINSON N., *Theory of Ordinary Differential Equations* (McGraw-Hill, New York) 1955.
- [23] STROGATZ S. H. and MIROLLO R. E., *J. Stat. Phys.*, **63** (1991) 613.
- [24] ACEBRÓN J. A. *et al.*, *Phys. Rev. E*, **57** (1998) 5287.
- [25] MONTBRIÓ E., KURTHS J. and BLASIUS B., *Phys. Rev. E*, **70** (2004) 056125.
- [26] BONILLA L. L. *et al.*, *Phys. Rev. Lett.*, **81** (1998) 3643.
- [27] ARIARATNAM J. T. and STROGATZ S. H., *Phys. Rev. Lett.*, **86** (2001) 4278.
- [28] HAN S. K., KURRER C. and KURAMOTO Y., *Phys. Rev. Lett.*, **75** (1995) 3190.
- [29] PIKOVSKY A. and ROSENBLUM M., *Physica D*, **240** (2011) 872.